

# IMPEDANCE AND INSTABILITIES FOR THE ALBA STORAGE RING

T.F. Günzel, F.Perez, CELLS, Bellaterra, Spain

## Abstract

The geometrical impedance in all 3 planes for most of the vacuum chamber elements of the ALBA storage ring was computed with the 3D-solver GdfidL[1]. Optimisation of some element geometries was carried out in order to reduce dissipative losses and in general, the impedance. Resistive wall impedance was calculated analytically. The thresholds of various instabilities were determined on the basis of analytically formulated threshold criteria. The most important are the transverse resistive wall instability and a HOM-driven longitudinal multibunch instability. It is proposed to combat the first one by a transverse feedback system and the second one by Landau damping.

## INTRODUCTION

ALBA is a synchrotron radiation facility which is currently under construction in Cerdanyola del Vallès near Barcelona. Its management is done by CELLS, a consortium co-financed by the Spanish and Catalan government. As a third generation light source it will produce high brilliant photon beams on a maximal number of 33 possible beamlines (including dipole beam lines). The project started in 2004 and is expected to run in user operation in 2010.

## VACUUM CHAMBER DESIGN

The storage ring has a very compact design due to its relatively small circumference of 268m and its large number of straight sections. It is designed to reach a current of 400mA. Its optics is realized by an expanded DBA-lattice with a total of 4 superperiods. They are connected with each other by 4 long straight sections of 8m. Each superperiod contains 3 middle long straight sections of 4.2m and 2 short straight sections of 2.6m.

The standard vacuum chamber, of octagonal shape, is of  $2a=72\text{mm}$  horizontal without considering the possible nose and  $2b=28\text{mm}$  vertical extension and is connected in most cases to an antechamber by a slot of 10mm in most cases. The chambers are normally of stainless steel (SS), for some low-gap chambers NEG-coated Al-chambers are foreseen. Most of the chambers are equipped with lumped absorbers. They are crotches horizontally inserted in the antechamber and always combined with a vertical pumping port. Additionally some distributed absorbers in front of the cavities, the low-gap chambers and the dipole chambers are installed[2].

## COMPUTATION OF THE IMPEDANCE

Consequently the storage ring has a large resistive wall (RW) impedance as well as a significant geometrical impedance due to the numerous low-gap chambers and other devices. In the following both types of impedance

will be distinguished due to the different way of their computation.

## Transverse resistive wall impedance

The computation of the RW-impedance is done analytically under the following simplifying conditions:

- The vacuum chamber wall is infinitely thick.
- Only the low-frequency range  $\omega \ll c(Z_0\sigma/b^2)^{1/3}$  is considered ( $c$  speed of light,  $\sigma$  conductivity,  $Z_0=376.73\Omega$ ) because of  $\sigma_\tau=15.4\text{ps}$  bunch length.
- The vacuum chamber can be considered as flat parallel plate geometry. Under this assumption according to [3] the only parameter characterising the dependence of the transverse impedance on geometry is the vertical extension of the chamber.
- The impedance of an element is weighted by its local  $\beta$ -function.

The first 2 conditions are usually fulfilled except for the NEG-coated Al-chambers and chambers with walls covered by thin metallic sheets or layers which are treated apart. 2 configurations will distinguished: The so-called phase I describes the status of the storage ring with 7 low-gap chambers (3 in-vacuum undulators, 3 8mm NEG-coated Al-chambers and one SS-chamber with a gap of 8.5mm) installed and the worst case which prospects an occupation of 10 middle straight sections with in-vacuum undulators at 6mm gap and the remaining middle and long straight sections with 8mm SS-chambers. This case is a simplification of the future, but demonstrates well what will happen if unconsideredly chambers of very small gap are installed.

## Transverse geometrical impedance

The geometrical impedance is computed numerically by element-wise wakefield evaluation with the 3D-code GdfidL (Only the impedance of the pump slits was estimated by analytical calculation.). For many vacuum chamber elements the transverse wakefields are calculated and decomposed in their monopolar, dipolar and quadrupolar part. The dipolar part is used to determine the transverse impedance. As for the RW-impedance the impedance values are weighted by the local  $\beta$ -function. For the worst case only one type of low-gap chambers was assumed to be installed in all straight sections. The spectra of vertical and horizontal impedance were determined and are depicted in the figure 1. Under the assumption that the transverse mode  $m=0$  meets the transverse mode  $m=-1$  after a coherent tune shift of one synchrotron tune, the impedance values result in the transverse mode-coupled instability (TMCI)-thresholds for single bunch (given in table 1) taking both the resistive and geometrical impedance into account.

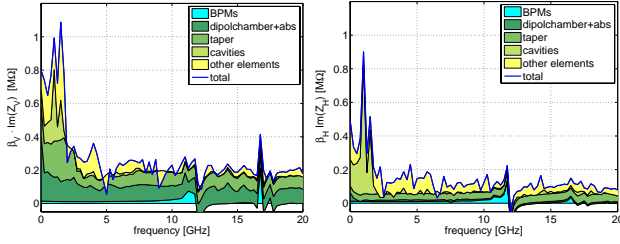


Fig.1: spectra of imaginary part of the  $\beta$ -weighted vertical(left) and horizontal(right) geometrical impedance for the phase I

Table 1: effective transverse impedances and threshold currents of TMC- and RW-instability

	Phase I	Worst case
$(Z_V\beta_V)^{RW}_{eff} [k\Omega]$	477	1497
$(Z_H\beta_H)^{RW}_{eff} [k\Omega]$	186	1139
$(Z_V\beta_V)^{geo}_{eff} [k\Omega]$	398	674
$(Z_H\beta_H)^{geo}_{eff} [k\Omega]$	174	273
$I_{RW}^V [mA]$	32.6	10.4
$I_{RW}^H [mA]$	126	20.6
$I_{TMCI}^V [mA]$	22.1	8.9
$I_{TMCI}^H [mA]$	53.7	13.7

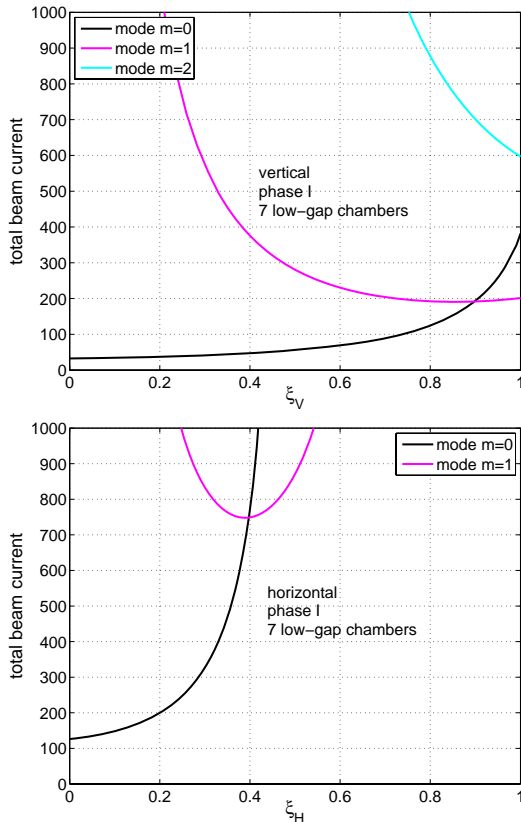


Fig. 2: resistive wall thresholds as function of normalized chromaticity on the vertical (above) and on the horizontal (below) plane for the lowest three modes.

## Longitudinal impedance budget

The RW and geometrical part of the longitudinal impedance are calculated as already explained. The RW part of the reduced longitudinal impedance  $Z_l/n$  ( $n=\omega/\omega_0$ ,  $\omega_0$  angular revolution frequency) amounts in the worst case (for simplicity only this case will be considered.) to:  $(Z_l/n)_{eff}=148m\Omega$ . The corresponding figure of the geometrical impedance was obtained by fitting several broadband resonator functions to the spectrum of the geometrical longitudinal impedance. The parameters of the fit are used to calculate the effective impedance by the following expression ( $R_{sk}$  shunt impedance,  $Q_k$  quality factor and  $\omega_{rk}$  resonance frequency of the  $k$ -th broadband resonator,  $\sigma_\tau$  bunch length in sec):

$$\left| \frac{Z_l}{n} \right|_{eff} = \sum_k \frac{R_{sk} \omega_0}{Q_k \omega_{rk}} \cdot g(\omega_{rk} \sigma_\tau)$$

with  $g(\omega\sigma_\tau)=2(\omega\sigma_\tau)^2$  for  $\omega\sigma_\tau \ll 1$  and  $g(\omega\sigma_\tau)=1$  for  $\omega\sigma_\tau > 1$ . The formfactor  $g$  weights resonators with low resonance frequency only weakly so that only resonators with high frequency can drive the microwave instability. The total value of  $|Z_l/n|_{eff}=424m\Omega$  is well below the threshold value of  $750m\Omega$  provided by the Boussard criterium[4] for the current of  $0.9mA$  in homogeneous filling. Even for 2/3-filling at full current the impedance value will not exceed the threshold and not excite the microwave instability.

## OPTIMISATION OF CHAMBER DESIGN

In order to limit power losses and hence the longitudinal impedance the design of several vacuum chambers was improved. GdfidL computations showed that the transition to the in-vacuum undulator which uses finger bearings hooked to the magnetic structure (adapted ESRF design[5]) at  $400mA$  homogenous filling produces power losses up to  $80W$  which would require cooling for the taper. However, by using a completely linear taper as at the SLS[6] these losses could be reduced by roughly a factor of 10. The higher current of ALBA compared to the ESRF created the need for this development.

The addition of connection bars above and below the beam in the design of horizontal stripline kicker reduced the power loss by a factor of 3 and the vertical impedance by almost a factor of 4. Design optimisation was also applied on flanges, absorbers and BPMs[7].

## RESISTIVE WALL INSTABILITY

It is the most menacing instability for ALBA. Already the RW-instability thresholds in phase I (table 1) are low and will decrease steadily with the installation of low-gap chambers. The use of a higher normalized chromaticity  $\xi=(\Delta Q_\beta/Q_\beta)/(\Delta E/E)$  only has a very limited effect (figure 2). In comparison to other synchrotron light sources the ratio of the head-tail phase to the normalized chromaticity at ALBA is quite small. Furthermore, the counteracting effect of a broadband component at higher frequency in the spectrum which is created by the geometrical impedance is very weak. Nevertheless, as only the

threshold of the  $m=0$  mode limits the current on the horizontal plane, it might be possible to combat this instable mode via Landau damping. But the necessary betatron spread would require several strong octupole magnets[8]. Otherwise the only solution to avoid the RW-instability is the foreseen installation of a transverse feedback system.

## DAMPING OF HOMs IN THE CAVITIES

As radio-frequency system a set of 6 warm copper cavities with HOM-dampers is foreseen[9]. Nevertheless there exists a HOM in the cavity which is not sufficiently damped. Its threshold is in homogeneous filling at 425mA corresponding to a shunt impedance of  $R_s=10.8k\Omega$ . Although the found threshold value is above the maximal current at ALBA, it could fall below 400mA in the final version of the cavities due to a slight variation of the shunt impedance. This instability can be damped by synchrotron tune spread via Landau damping. This one could for instance be created by the installation of a harmonic cavity. However, according to a model developed at the ESRF[10], 2/3-filling already produces enough synchrotron frequency spread in the ALBA ring to provide Landau damping of the HOM. This is inasmuch interesting as the sensitivity of a compact medium energy ring to longitudinal coupled instabilities is 5 times larger than at a larger accelerator as the ESRF. The sensitivity  $S$  [11] can be expressed in the following way by standard machine parameters ( $\alpha$  momentum compaction factor,  $\tau_L$  longitudinal damping time,  $E$  energy,  $e$  elementary charge and  $Q_s$  synchrotron tune):  $S=\alpha\tau_L/(2(E/e)Q_s)$ . On the other hand, the HOM-threshold at zero synchrotron frequency spread can be expressed in the following, very instructive way (with  $f_{HOM}$  as frequency and  $Z_{HOM}$  as shunt impedance of the HOM):

$$I_{thres}(\Delta f_s = 0) = \frac{1}{S f_{HOM} Z_{HOM}}$$

The threshold current is 4.4 times higher than at the ESRF since the value of  $Z_{HOM}$  is very small because the ALBA-cavities are (supposed to be) HOM-damped. The HOM in the cavities is much weaker than corresponding one in the ESRF cavities. Therefore it is also easier to damp it with Landau damping. Therefore although the synchrotron spread due to 2/3 filling in the ALBA-ring is indeed 6 times smaller than the corresponding spread in the ESRF-ring, (because of a smaller value of the R/Q of the fundamental mode of ALBA), this spread is already sufficient to shift the threshold of the HOM from 425mA to 476mA. Figure 3 shows how the threshold current depends on the level of fractional filling for different values of shunt impedance of the HOM.

## CONCLUSION

The ALBA ring is prone to instabilities due to its compact design and high operation current. The strong resistive wall instability can be cured on the vertical and horizontal plane by a transverse feedback system.

However, due to relatively small vertical size of the standard vacuum chamber and the low  $\beta$ -functions the total value of the geometrical transverse impedance is only moderate. The unexpected presence of the E011-mode based HOM in the cavities can be damped in the starting phase by 2/3- filling of the ring and on a later stage by the installation of a harmonic cavity. Even in this filling pattern the microwave instability will probably not be excited. The vacuum chamber elements are supposed to withstand the 50% higher heat load in this filling mode.

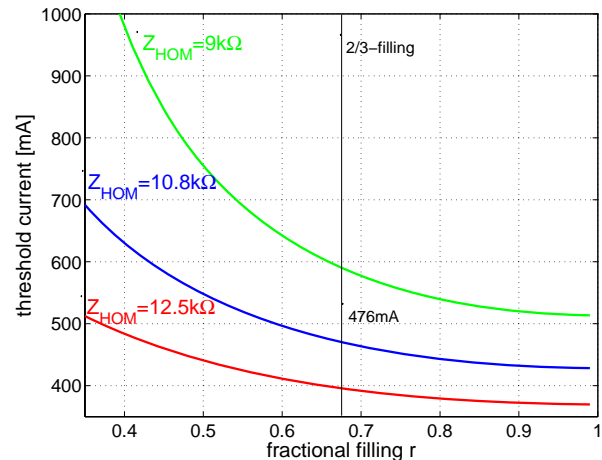


Fig.3: threshold due to Landau damping as a function of fractional filling and HOM shunt impedance  $Z_{HOM}$ . At  $r=0.66$  and  $Z_{HOM}=10.8k\Omega$  the threshold reaches 476mA.

## REFERENCES

- [1] W. Bruns, 3D code GdfidL, www.gdfidL.de
- [2] E. Al-Dmour et al., "The vacuum system for the Spanish synchrotron light source ALBA", EPAC'06, Edinburgh, p.3398
- [3] K. Yokoya, "Resistive wall impedance of Beam Pipes of General Cross Section", Part. Acc. 41 (1993), 221
- [4] A. Chao, "Physics of collective Beam instabilities in high energy accelerators", J.Wiley & Sons, NY(1993)
- [5] J.Chavanne et al., "Construction of Apple II and in-vacuum undulators at ESRF", PAC01, Chicago p.2459
- [6] G. Ingold et al., "Performance of Small-Gap Undulators at SLS intermediate Energy Storage Ring", SRI 2006, Korea
- [7] A. Olmos et al., "BPM design for the ALBA synchrotron", EPAC'06, Edinburgh, p.1190
- [8] J.Gareyte et al., "Landau damping, dynamic aperture and octupoles in the LHC", LHC project 91 (revised), CERN, (1997)
- [9] F. Perez et al., "New developments for the RF-system of the ALBA storage ring", EPAC'06, Edinburgh, p. 1346
- [10] O. Naumann, J.Jacob, "Fractional Filling induced Landau damping of longitudinal instabilities at the ESRF", PAC'97, Vancouver, p.1551
- [11] A.Mosnier, "Cures of coupled bunch instabilities", PAC'99, NY, p.628